

H_3^+ in dense and diffuse clouds

Benjamin J. McCall,^{a*} Kenneth H. Hinkle,^b Thomas R. Geballe^c and Takeshi Oka^a

^a Department of Astronomy and Astrophysics, Department of Chemistry, and the Enrico Fermi Institute, The University of Chicago, Chicago, IL 60637, USA

^b National Optical Astronomy Observatories, Tucson, AZ 85726, USA

^c Joint Astronomy Centre, University Park, Hilo, HI 96720, USA

Interstellar H_3^+ has been detected in dense as well as diffuse clouds using three 3.7 μm infrared spectral lines of the ν_2 fundamental band. Column densities of H_3^+ from $(1.7\text{--}5.5) \times 10^{14} \text{ cm}^{-2}$ have been measured in dense clouds in absorption against the infrared continua of the deeply embedded young stellar objects GL2136, W33A, MonR2 IRS 3, GL961E, and GL2591. Strong and broad H_3^+ absorptions have been detected in dense and diffuse clouds towards GC IRS 3 and GCS3-2 in the region of the galactic center. A large column density of H_3^+ , comparable to that of a dense cloud, has been detected towards the visible star Cygnus OB2 No. 12, which has a line of sight that crosses mostly diffuse clouds. The H_3^+ chemistry of dense and diffuse clouds are discussed using a very simple model. Some future projects and problems are discussed.

1 Background

Protonated hydrogen, H_3^+ , is the simplest stable polyatomic molecule, and was discovered in 1911 by J. J. Thompson.¹ It is the most abundant ion in hydrogen plasmas, as initially discovered by A. J. Dempster.² In 1925, Hogness and Lunn³ introduced the celebrated ion–neutral reaction



as the primary mechanism for H_3^+ production. By the 1930s, the predominance of H_3^+ among cations in hydrogen plasmas was well established experimentally,⁴ and the systematic theoretical studies by Eyring, Hirschfelder and others had explained the large cross-section⁵ and high exothermicity⁶ of reaction (I). Readers are referred to a review⁷ for more details of early works.

1.1 Interstellar H_3^+

The 1961 paper by Martin *et al.*⁸ seems to be the first to suggest that H_3^+ should be abundant in interstellar space. In 1970, Stecher and Williams⁹ discussed the production and destruction rates of interstellar H_3^+ . The first numerical estimate of the interstellar H_3^+ concentration was reported by Solomon and Werner,¹⁰ who also took the decisive step of introducing the cosmic ray as the major agent of ionization. Their estimate of the H_3^+ fraction $X(\text{H}_3^+) \equiv [\text{H}_3^+]/[\Sigma\text{H}] \approx 10^{-6}$ (where $[\Sigma\text{H}]$ denotes the total number density of hydrogen atoms), can be contrasted to the value 10^{-8} derived in this paper. de

Jong¹¹ did similar calculations and obtained $X(\text{H}_3^+) \approx 0.4\text{--}1.0 \times 10^{-6}$. Reaction (I) was also used by Glassgold and Langer¹² as the mechanism for cosmic ray heating of molecular clouds and by Watson¹³ in his theory of isotope fractionation in interstellar HD.

In 1973, the science of interstellar H_3^+ acquired a new dimension, when Watson¹⁴ and Herbst and Klemperer¹⁵ independently proposed a network of ion–neutral reactions as the mechanism to generate the wide variety of simple molecules that had been observed in interstellar space by radioastronomers.¹⁶ This idea, which was perhaps influenced by the millimeter wave detection of X-ogen by Buhl and Snyder¹⁷ and its subsequent identification as HCO^+ by Klemperer,¹⁸ revealed that H_3^+ plays a central role in interstellar chemistry. Because of the relatively low proton affinity of H_2 (4.5 eV), H_3^+ protonates practically all atoms and molecules through the general reaction



(He, Ne, Ar, N and O_2 are notable exceptions). After protonation, the HX^+ combines with other species through the reaction



and initiates a network of chemical reactions. The detailed numerical model calculation of such networks in the classic paper by Herbst and Klemperer¹⁵ explained many of the observed results. Their success triggered an avalanche of papers and reviews on interstellar chemistry based on the ion–neutral reaction scheme. While they are too numerous to cite, many important papers can be traced from the references given in three works that were essential in the preparation of this discussion: the paper by de Jong *et al.*¹⁹ on H_3^+ chemistry, the chemical model calculation for diffuse clouds by van Dishoeck and Black,²⁰ and the model for dense clouds by Lee *et al.*²¹

1.2 The search for H_3^+

‘It is likely that H_3^+ is present in the interstellar medium, since H_2^+ ions must be formed from the H_2 molecules present in the interstellar medium either by light absorption beyond 805 Å or by cosmic rays and since each H_2^+ ion will, upon collision with a neutral H_2 molecule, immediately form H_3^+ according to reaction (I). However, the possibility of detecting H_3^+ in interstellar space depends on the discovery of a spectrum of this molecule in the laboratory.’

Gerhard Herzberg, 1967²²

Herzberg thus attempted together with J. W. C. Johns to observe the infrared ν_2 fundamental band of H_3^+ in emission. Since H_3^+ does not have well-bound electronic excited states,⁷ no ultraviolet or visible spectrum is expected. Its symmetric equilateral triangle structure also forbids a conventional rotational spectrum. Therefore, the infrared active degenerate ν_2 band is the most straightforward way to detect interstellar H_3^+ .

There were other proposals based on radioastronomy, which is by far the most sensitive method of detecting interstellar molecules. Salpeter and Malone²³ pointed out the possibility of detecting H_3^+ using its radio recombination lines, which are slightly shifted from the H^+ recombination lines due to the difference in reduced mass. The recombination lines of He^+ and C^+ were well known. An emission line feature was noted between the $85\alpha\text{H}^+$ and $85\alpha\text{He}^+$ in NGC2024²⁴ but its frequency was not quite right.²⁵ The detection of H_3^+ using this technique is probably very difficult because of the low abundance of H_3^+ in H II regions, where recombination lines are strong.

Another proposal²⁶ was to detect the deuterated species H_2D^+ . The deuteration shift of the center of gravity from the center of charge produces an effective dipole moment of 0.6 D and makes the rotational spectrum active in the radio and far-infrared region. The abundance of H_2D^+ is much higher than expected from the natural abun-

dance of deuterium because of the efficient isotope fractionation, first explained by Watson.^{13, 27} A detection of H_2D^+ emission at 372 GHz was reported²⁸ in NGC2264 but was later negated.²⁹ A more recent detection of an H_2D^+ signal by Boreiko and Betz³⁰ in absorption at 1370 GHz in Irc2 has a better signal-to-noise ratio, though its authenticity has yet to be confirmed. The search for interstellar H_3^+ using its centrifugal distortion spectrum³¹ was noted³² and advocated by Draine and Woods³³ for studies of high temperature objects such as the X-ray heated clouds NGC6240.

The most straightforward way of searching for H_3^+ became possible in 1980 when its infrared ν_2 band spectrum was discovered in the laboratory.³⁴ An immediate attempt to detect H_3^+ in the Becklin–Neugebauer (BN) source in Orion using the FTIR spectrometer at the 4 m Mayall Telescope of the Kitt Peak National Observatory (KPNO) was unsuccessful.³⁵ A search by two of the authors (T.R.G. and T.O.) was continued using a Fabry–Perot interferometer and a generation of cooled grating spectrometers (CGS) at the UK Infrared Telescope (UKIRT) on Mauna Kea, during which negative results for several sources were published.³⁶ The search was also attempted by many other groups and some of them published their inconclusive results.^{37–40}

From 1988 to 1994, our observational work was diverted to studying H_3^+ in planetary ionospheres following the discovery of strong H_3^+ emission in the auroral regions of Jupiter, Saturn and Uranus,⁴¹ as well as the Comet SL-9 impact on Jupiter. During this time the resolution, sensitivity and reliability of observational infrared spectrometers improved dramatically—a major factor in this development was the use of infrared detector arrays. In 1994, an infrared absorption line of H_2 in NGC2024 was detected at the NASA Infrared Telescope Facility (IRTF).⁴² This detection suggested that the sensitivity of IRTF's CSHELL spectrometer had reached the point necessary for H_3^+ detection, since it was known³⁵ that the ratio of the intensities of the H_3^+ dipole transition and the H_2 quadrupole transition ($\approx 10^9$) just about cancelled the abundance ratio of H_3^+ to H_2 ($\approx 10^{-9}$). Our applications for observing time using CSHELL on IRTF were rejected for three consecutive terms, and interstellar H_3^+ was instead detected by the CGS4 spectrometer at UKIRT, in 1996. Since then our observations have progressed, yielding positive detections in dense clouds, diffuse clouds, and in the region of the galactic center.

2 The H_3^+ spectrum

Since the details of the ν_2 fundamental band vibration–rotation spectrum were given in a recent Faraday Discussion,⁴³ here we simply note two characteristics of the H_3^+ spectrum: the vibrational frequency and the rotational level structure. Both of these characteristics have important consequences for the observation of interstellar H_3^+ .

2.1 Vibrational frequency

When a proton is added to an H_2 molecule, the extra charge pushes the two protons away and the equilibrium interproton distance increases from 0.74 Å to 0.87 Å. The vibrational frequency is reduced from 4161.2 cm^{-1} to $\nu_1 = 3178.3 \text{ cm}^{-1}$ ⁴⁴ and $\nu_2 = 2521.3 \text{ cm}^{-1}$.⁴⁵ The infrared active ν_2 band is located in a region free from spectral lines of ordinary molecules made from atoms with high cosmic abundance. The hydrogen stretching vibrations of C–H, N–H and O–H bonds are all much higher in frequency and even the high J P-branch lines of light molecules, such as CH_4 , NH_3 and H_2O , do not reach the 4 μm region. The hydrogen bending vibrations are all too low in frequency and their R-branches do not reach this region. The stretching vibrations of heavier elements such as C=O, C \equiv N and C \equiv C are the closest to this region, but their rotational structures do not extend much in frequency because of their larger moments of inertia. Fig. 1, which was adapted from Genzel's review,^{46,47} shows the unique position

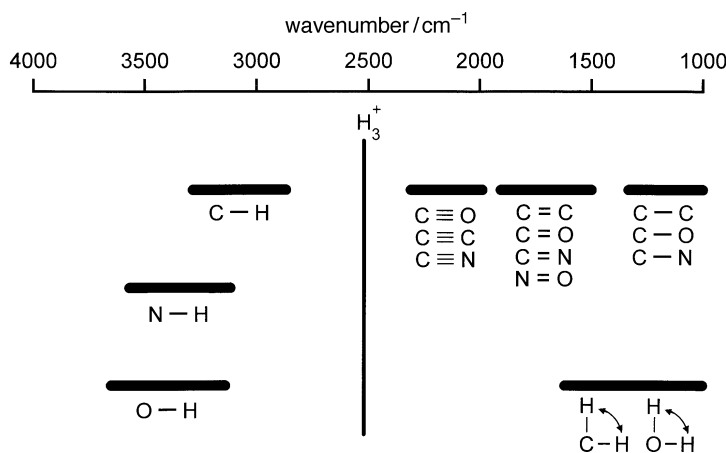


Fig. 1 Position of the ν_2 band of H_3^+ compared with other common molecular vibrations. Note that H_3^+ is relatively free of interference from spectral lines of ordinary molecules made from atoms with high cosmic abundance. This figure is adapted from Genzel's review.^{46,47}

of the H_3^+ ν_2 band. This freedom from the spectra of other molecules is the reason for the extremely pure H_3^+ emission spectrum of Jupiter reported by Maillard *et al.*⁴⁸ More importantly for observations of interstellar H_3^+ , this favored location of the band origin makes our ground-based observation relatively unhindered by interference with molecules in the terrestrial atmosphere (L window). The only spectral lines that interfere with our observations are deuterium stretching vibrations, notably of HDO, and overtone and combination bands, notably of the $\nu_2 + \nu_4$ band of CH_4 , which are of course orders of magnitude weaker than the fundamental bands. Had the ν_2 band appeared in the 3 μm region, it would have been next to impossible to detect interstellar H_3^+ from ground-based observatories.

2.2 Rotational level structure

Because of its small mass, H_3^+ has large rotational constants⁴⁵ $B = 43.56 \text{ cm}^{-1}$ and $C = 20.61 \text{ cm}^{-1}$, and only the lowest few levels are significantly populated in molecular clouds with temperatures of 10–100 K. The structure of the lowest rotational levels is shown in Fig. 2, where the energy scale is expressed in temperature (Kelvin). J is the rotational angular momentum quantum number and K is its projection onto the C_3 symmetry axis. A special characteristic of this rotational structure is that the lowest level with $J = K = 0$ (shown in Fig. 2 with a broken line) is not allowed by the Pauli exclusion principle. According to Dirac's statement of the Pauli principle,^{49,50} the total wavefunction must change sign when two protons are interchanged but must remain invariant when the three protons are cyclicly permuted. The wavefunction of the lowest rotational level is simply a constant and these conditions cannot be simultaneously satisfied, whether this rotational wavefunction is combined with the *ortho* nuclear spin function (in which all proton spins are parallel, $I = \frac{3}{2}$, and the first condition is not satisfied) or with the *para* nuclear spin function (in which one proton spin is antiparallel, $I = \frac{1}{2}$, and the second condition is not satisfied).

This leaves the $J = 1, K = 1$ level of *para*- H_3^+ as the lowest ground rotational level. This and the next lowest level with $J = 1, K = 0$ of *ortho*- H_3^+ , which is higher than the ground level by 32.9 K, are the only levels that are significantly populated for temperatures of 5–50 K. These two levels contain nearly equal populations of molecules,

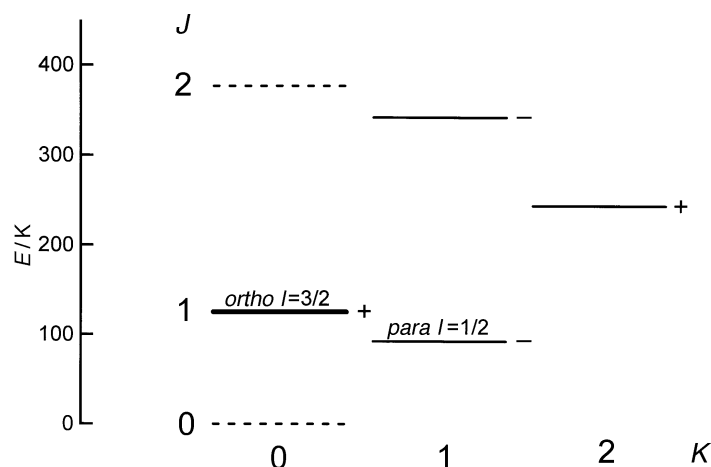


Fig. 2 Structure of the lowest rotational levels of H_3^+ . Broken lines represent forbidden levels, the bold line indicates a level with the *ortho* ($I = \frac{3}{2}$) spin modification, the thin lines indicate levels with the *para* ($I = \frac{1}{2}$) spin modifications. The (+) and (-) signs indicate the parity of the levels. The transitions studied in interstellar space arise from the $J = 1$ levels.

since the higher spin statistical weight of *ortho*- H_3^+ ($g_I = 2I + 1 = 4$) than that of *para*- H_3^+ ($g_I = 2$) is approximately compensated for by the Boltzmann factor $\exp(-32.9/T)$. We thus have six spectral lines of comparable intensities at 30 K as shown in Fig. 3, two from *ortho*- H_3^+ [$\text{R}(1,0)$ and $\text{Q}(1,0)$] and four from *para*- H_3^+ [$\text{R}(1,1)^+$, $\text{R}(1,1)^-$, $\text{Q}(1,1)$ and $\text{P}(1,1)$]. The existence of six lines makes the observation flexible—we may choose lines that are freest from the telluric interference depending on the weather and the Doppler shift of the night. Two of the spectral lines, $\text{R}(1,1)^+$ of *para*- H_3^+ and $\text{R}(1,0)$ of

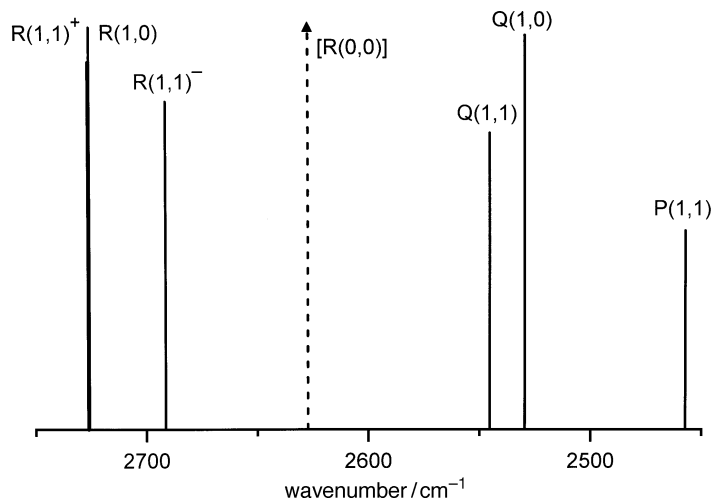


Fig. 3 Six available spectral lines of the ν_2 band of H_3^+ . Note that $\text{R}(1,1)^+$ and $\text{R}(1,0)$ form a doublet with spacing of 0.321 cm^{-1} , which is particularly useful for astronomical observations. The broken line marks the hypothetical position of the transition arising from the forbidden level $J = K = 0$. This line would have an intensity four times that of the other strongest lines if it were allowed. These intensities are calculated for an assumed temperature of 30 K.

ortho- H_3^+ , are separated by only 0.321 cm^{-1} and are particularly useful for the measurement of temperature and for confirmation of detections.

Had the lowest $J = K = 0$ level been allowed, the spectrum of H_3^+ would be like an atomic spectrum, since most of the molecules would be in the lowest level, and the R(0,0) line would be the only strong line, at the position shown with a broken arrow in Fig. 3.

3 Observed results

Observations of interstellar H_3^+ have so far been conducted using three infrared spectrometers: the CGS4 at UKIRT with spectral resolution $R \approx 20\,000$, the Phoenix spectrometer at KPNO with $R \approx 60\,000$, and the CSHELL at NASA IRTF with $R \approx 20\,000$. All of them have produced positive results. Interstellar H_3^+ has been found in gravitationally bound dense clouds with high density ($[\Sigma H] \approx 10^3\text{--}10^5\text{ cm}^{-3}$) as well as in unbound diffuse clouds with low density ($10\text{--}10^3\text{ cm}^{-3}$).

3.1 H_3^+ in dense clouds

The first spectra of interstellar H_3^+ were detected towards the young stellar objects (YSOs) GL2136 and W33A, which are deeply embedded in dense molecular clouds.⁵¹ These spectra were obtained with CGS4 at UKIRT on the nights of April 25, June 10 and July 15, 1996. These YSOs were chosen because of their infrared brightness and because of their large column densities of foreground gas. In addition, it was thought advantageous⁵² to use carbon depleted clouds where H_3^+ is destroyed less by the proton hop reaction (II). Strong absorptions of solid CO frozen on dust grains have been reported^{53,54} although the depletions might not be large.⁵⁵

The R(1,0)–R(1,1)⁺ doublet of H_3^+ mentioned earlier was used for the detection. The observed signal to noise ratios of the absorption lines were by no means great, but the Doppler shift of the doublet lines due to the earth's orbital motion from April 25 to July 15 convinced us that the signals were genuine (see Fig. 4).

Subsequent observations revealed interstellar H_3^+ in dense clouds towards three other YSOs: MonR2 IRS 3 and GL961E (February 11–14, 1997, at UKIRT), and

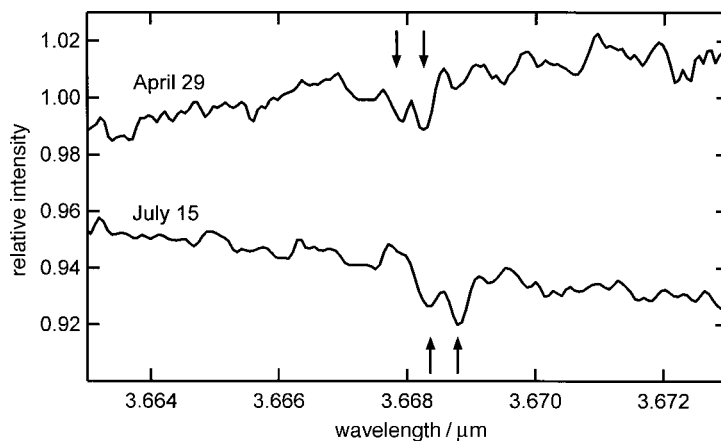


Fig. 4 Spectra of the R(1,0)–R(1,1)⁺ doublet of H_3^+ obtained with the CGS4 spectrometer at UKIRT along the line of sight to GL2136. The upper trace was obtained on 29 April, 1996, while the lower trace was obtained on 15 July, 1996. The observed Doppler shift of the doublet (marked with arrows) between the two dates matches that expected from the Earth's orbital motion, providing convincing evidence that the doublet is genuine.

GL2591 (July 11–12, 1997, at UKIRT). The observed equivalent widths W_ν yield the H_3^+ column densities using the standard formula

$$W_\nu \equiv \int [\Delta I(\nu)/I(\nu)] d\nu = (8\pi^3\nu/3hc)N|\mu|^2 \quad (1)$$

where $|\mu|^2$ is the square of the transition dipole moment. The spectral lines of *ortho*- H_3^+ and *para*- H_3^+ give their column densities N_o and N_p separately, and their sum gives the total H_3^+ column density $N(\text{H}_3^+)$. The ratio of N_o and N_p gives the temperature of the clouds using the standard formula

$$\frac{N_o}{N_p} = \frac{g_o}{g_p} e^{(-\Delta E/kT)} = 2 e^{(-32.9/T)} \quad (2)$$

These results are summarized in Table 1. We have also studied the infrared sources GL490, GL989, LkH α 101, MonR2 IRS 2, M17 IRS 1, S140 IRS 1, W3 IRS 5, Elias 29, NGC2024 IRS 2 and BN. So far, our data reduction has not provided evidence of column densities at the level of *ca.* $2\text{--}3 \times 10^{14} \text{ cm}^{-2}$, but careful reprocessing of these spectra continues. The lack of strong H_3^+ absorption towards NGC2024 IRS 2 and BN was particularly surprising in view of the large column density of H_2 reported in the former⁴² and the observed richness of molecules in the latter. We believe that these non-detections are not due to the absence of H_3^+ in the clouds but are simply due to the short column length of the clouds in front of the source (see the discussion in Section 4.1). More details of our study of dense clouds will be published elsewhere.⁵⁶

3.2 H_3^+ in diffuse clouds

During our survey of H_3^+ in dense clouds, we observed strong and broad H_3^+ absorption signals in the direction of the infrared sources GC IRS 3 and GCS3-2 (July 11–12, UKIRT), in the region near the galactic center. These sources are thought to be 8 kpc away and their lines of sight may cross several clouds, both dense and diffuse. Indeed McFadzean *et al.*⁵⁷ reported observational evidence for two components in the extinction: the 3.0 μm ice absorption (a signature of dense clouds) and the 3.4 μm hydrocarbon absorption (a signature of diffuse clouds). More details of our galactic center observations will be published separately.⁵⁸

The galactic center results led us to try Cygnus OB2 No. 12, a visible star with high extinction discovered in 1954.⁵⁹ It is generally believed that this star is obscured largely by diffuse, low density clouds containing little molecular material.⁶⁰ We clearly observed

Table 1 Positions and derived column densities and temperatures for H_3^+ sources

infrared source	position		$N(\text{H}_3^+)/ (10^{14} \text{ cm}^{-2})^a$	T/K
	α (1950)	δ (1950)		
dense clouds				
GL2136	18 : 19 : 36.6	−13 : 31 : 40	3.6 ± 0.6	35 ± 4
W33A	18 : 11 : 44.2	−17 : 52 : 56	5.5 ± 1.9	30 ± 6
MonR2 IRS 3	06 : 05 : 21.8	−06 : 22 : 26	2.1 ± 0.7	24 ± 4
GL961E	06 : 31 : 59.1	+04 : 15 : 10	1.7 ± 0.7	24 ± 5
GL2591	20 : 27 : 35.8	+40 : 01 : 14	2.0 ± 1.0^b	
diffuse clouds				
Cyg OB2 No. 12	20 : 30 : 53.4	+41 : 03 : 52	3.8 ± 0.5	20 ± 4

^a Statistical uncertainties (3σ) are quoted in parentheses but systematic errors are difficult to estimate and might be larger. ^b Estimated systematic uncertainty is given for GL2591, as this spectrum is not yet fully reduced.

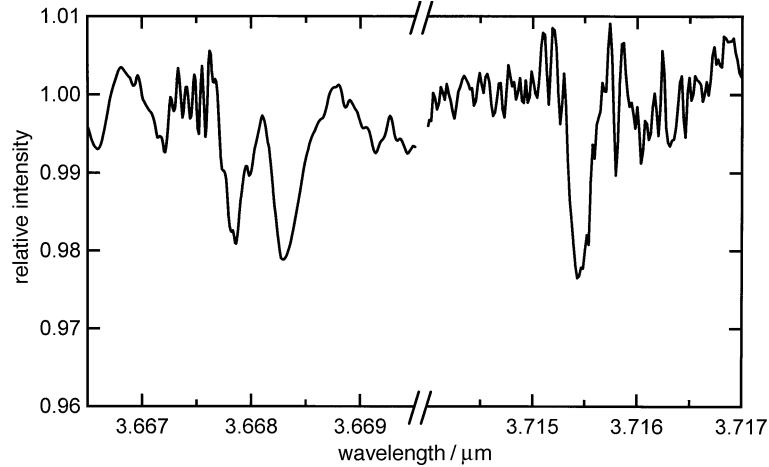


Fig. 5 Spectra of the line of sight towards the visible star Cygnus OB2 No. 12. The left trace, showing the $\text{R}(1,0)$ – $\text{R}(1,1)^+$ doublet of H_3^+ , was obtained with CGS4 at UKIRT on 11 July, 1997. The right trace, showing the $\text{R}(1,1)^-$ line of H_3^+ , was obtained with the new Phoenix spectrometer at KPNO on 17 September, 1997. The high frequency interference in the CGS4 spectrum near 3.6675 μm is due to the removal of a telluric CH_4 absorption line.

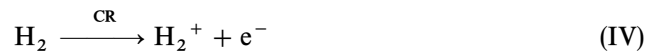
the H_3^+ $\text{R}(1,0)$ – $\text{R}(1,1)^+$ doublet (July 11–12, UKIRT) and the $\text{R}(1,1)^-$ singlet (September 15–17, KPNO),⁶¹ Because of the high humidity in Arizona in September, strong and wide telluric HDO lines (ν_2 band $1_{10} \leftarrow 1_{11}$ and $4_{22} \leftarrow 4_{23}$) made the observation of the doublet impossible, but the singlet (which has only CH_4 lines nearby) was clearly observed. The observed spectrum is shown in Fig. 5. Using the observed equivalent widths of the lines and eqn. (1), we obtain the remarkable result that the column density of H_3^+ in the direction of Cygnus OB2 No. 12 is $(3.8 \pm 0.5) \times 10^{14} \text{ cm}^{-2}$, comparable to that of the dense clouds listed in Table 1. van Dishoeck and Black^{20,62} reported their extensive chemical model calculation in diffuse clouds and predicted high column densities of H_3^+ , but their calculation was based on an extremely small electron recombination rate constant, which has since been demonstrated to be too low by more than three orders of magnitude.⁶³ Calculations given in the next section show that the large column density of H_3^+ in the diffuse clouds towards Cygnus OB2 No. 12 is due not to a high number density of H_3^+ but simply to a long column length. Our calculation is much cruder than that of van Dishoeck and Black but is essentially the same as far as the H_3^+ chemistry is concerned, except that a revised recombination rate is used.

4 H_3^+ chemistry

A very attractive aspect of H_3^+ as a molecular astronomical probe is its simple chemistry. The simplicity of the chemistry allows us to make relatively simple and reliable arguments about the H_3^+ number densities and other astrophysical quantities. In the following, we give a crude order of magnitude discussion of its chemistry; more detailed chemical model calculations such as those given by Lee *et al.*²¹ and by van Dishoeck and Black²⁰ are of course desirable for more accurate discussions.

4.1 H_3^+ chemistry in dense clouds

In cold dense clouds, which are protected from star radiation, H_3^+ is produced almost exclusively from the cosmic ray (CR) ionization of H_2 to H_2^+ ,



followed by the ion–neutral reaction (I). Reaction (I) is many orders of magnitude more rapid than reaction (IV) and the production rate is governed by the rate of reaction (IV), *i.e.*, $\zeta[\text{H}_2]$. The cosmic ray ionization rate $\zeta \approx 10^{-17} \text{ s}^{-1}$ and H_2 number density $[\text{H}_2] \approx 10^4 \text{ cm}^{-3}$ yield an H_3^+ production rate of *ca.* $10^{-13} \text{ cm}^{-3} \text{ s}^{-1}$.

H_3^+ is destroyed predominantly by the proton hop reaction (II). Equating the production and destruction rates, we have the steady-state equation

$$\zeta[\text{H}_2] = \sum_x k_x[\text{H}_3^+][\text{X}] \quad (3)$$

where k_x is the rate constant for reaction (II). Since CO is the most abundant molecule in dense clouds, we neglect the terms of the other atoms and molecules in eqn. (3) and obtain the H_3^+ number density

$$[\text{H}_3^+] = \frac{\zeta}{k_{\text{CO}}} \frac{[\text{H}_2]}{[\text{CO}]} \quad (4)$$

Since the ratio $[\text{H}_2]/[\text{CO}] \approx 10^4$ is approximately constant over a wide variety of molecular parameters,²¹ this shows that $[\text{H}_3^+]$ is constant. Using the Langevin rate⁶⁴ $k_{\text{CO}} \approx 10^{-9} \text{ cm}^3 \text{ s}^{-1}$ we obtain $[\text{H}_3^+] \approx 10^{-4} \text{ cm}^{-3}$. The observed H_3^+ column density of $3 \times 10^{-14} \text{ cm}^{-2}$ (see Table 1) gives a typical effective column length of $\approx 1 \text{ pc}$.

The most serious omission in this discussion is the neglect of X terms other than CO from eqn. (3). In the model calculations of Lee *et al.*,²¹ the abundance of O is predicted to be comparable to that of CO. Inclusion of the O term will reduce the $[\text{H}_3^+]$ by *ca.* 30% since the rate constant k_{O} is about 1/2.5 of k_{CO} .⁶⁴ The neglect of the electron term $\text{X} = \text{e}^-$ in eqn. (3) also has to be addressed since the recombination rate constant k_{e} is larger than k_{CO} by more than two orders of magnitude (see Section 4.2). However, the model calculations of Lee *et al.*²¹ show that this correction is significant only in clouds with high metallicity, where the electron concentration is increased by the ionization of alkali and alkaline-earth metals with low work functions. The lack of accurate measurements of k_{O} (and for that matter even of k_{CO}) is also a source of error and more laboratory studies are awaited.

However, all these corrections will be small compared to the large uncertainty in ζ . We hope that our H_3^+ measurements will help further constrain this important parameter.

4.2 H_3^+ chemistry in diffuse clouds

In diffuse clouds where the number density is low ($10\text{--}10^3 \text{ cm}^{-3}$) and visible light passes through, cosmic ray ionization followed by reaction (I) is again the primary mechanism for H_3^+ production. Photoionization of H_2 is not effective because the cloud contains abundant atomic H atoms whose ionization potential (13.6 eV) is lower than that of H_2 (15.4 eV).

The main destruction mechanism of H_3^+ in diffuse clouds is expected to be electron recombination, because of the high number density of electrons created by photoionization of carbon (the carbon atom has the lowest ionization potential, 11.3 eV, of any abundant species). We assume for simplicity that all carbon atoms which are not depleted onto dust grains are ionized and that all electrons come from the ionization of carbon atoms, *i.e.*, $[\text{e}^-] = [\text{C}^+] = [\Sigma\text{C}]$, where $[\Sigma\text{C}]$ denotes the total number density of carbon atoms. The solution of the steady state equation is then

$$[\text{H}_3^+] = \frac{\zeta}{k_{\text{e}}} \frac{[\text{H}_2]}{[\text{e}^-]} \quad (5)$$

indicating that the H_3^+ number density is constant also in diffuse clouds. Using $k_{\text{e}} \approx 10^{-7} \text{ cm}^3 \text{ s}^{-1}$ ⁶³ and $[\text{H}_2]/[\text{e}^-] \approx [\text{H}_2]/[\Sigma\text{C}] \approx 10^4$ we obtain an H_3^+ number

density of $[\text{H}_3^+] \approx 10^{-6} \text{ cm}^{-3}$, smaller than that of dense clouds by two orders of magnitude. Thus the same H_3^+ column density as in dense clouds ($3 \times 10^{14} \text{ cm}^{-2}$) implies an effective path length (L) that is longer by two orders of magnitude, $L \sim 100 \text{ pc}$. This path length is very likely composed of several diffuse clouds rather than a single cloud.

There is a major uncertainty in the above estimates, apart from that of ζ . Unlike other k_x with Langevin rates, which are independent of temperature,^{65,66} k_e varies significantly at low temperature. If we use $k_e = 4.6 \times 10^{-6}/T^{0.65} \text{ cm}^3 \text{ s}^{-1}$, as determined from the storage ring experiment of Sundström *et al.*,⁶⁷ and assume $T \approx 30 \text{ K}$, k_e is closer to $10^{-6} \text{ cm}^3 \text{ s}^{-1}$ and $L \approx 1 \text{ kpc}$. In addition, we have not considered direct photodissociation of H_3^+ . This is thought to be slow⁶⁸ but more theoretical and experimental studies are certainly needed.

4.3 Intermediate case

The above two analyses for the extreme cases can be generalized to the intermediate case where the destruction rates of H_3^+ by CO and by electrons are comparable. We assume that all carbon atoms in the gas phase are either in the form of C^+ or CO, that is, $[\Sigma\text{C}] = [\text{C}^+] + [\text{CO}]$, where $[\Sigma\text{C}]$ denotes the total number density of carbon atoms in any gaseous form. Other carbon species (atomic C, CO_2 , CH_4 , *etc.*) can be included in $[\text{CO}]$ since they all have Langevin rates for the proton hop reaction (II). We have

$$[\text{H}_3^+] = \zeta \frac{f}{2} \frac{[\Sigma\text{H}]}{[\Sigma\text{C}]} \left[\frac{1}{k_e(1-\alpha) + k_{\text{CO}}\alpha} \right] \quad (6)$$

where f is the fraction of hydrogen atoms in molecular form $f \equiv 2[\text{H}_2]/[\Sigma\text{H}]$ and α is the fraction of carbon atoms in molecular form, $\alpha \equiv [\text{CO}]/[\Sigma\text{C}]$. For derivation of this formula and further discussions of the total number density $[\Sigma\text{H}]$ and path length L of the cloud, see McCall *et al.*⁶¹

5 Future prospects

Our observations have established that interstellar H_3^+ exists with sufficient abundance to be observable from ground-based observatories both in dense and diffuse clouds. In fact, we find it easier to observe H_3^+ absorption lines than H_2 infrared absorption lines. Perhaps H_3^+ is not only a powerful probe for the study of plasma activities of astronomical objects, but also a most convenient probe for the detection of hydrogenic molecular species. In the spirit of this conference, we speculate in this section on some possible developments in the immediate future.

5.1 Future observations

From ground-based observatories, H_3^+ will be found in many other sources. For dense clouds the observations will give information of the depth of the embedded YSO and for diffuse clouds they will give the dimension of the clouds. For a source like the Quintuplet near the galactic center where many infrared sources are positioned within a narrow angle of sight, some type of 'mapping' such as radioastronomers do might be possible. This will be most efficiently done when the Phoenix spectrometer is moved to the Cerro Tololo Interamerican Observatory next year (1999). The expected advent of larger telescopes with high-resolution infrared spectrometers, such as Gemini and Subaru, and the installation of a high-resolution spectrometer at Keck will allow us to observe much fainter infrared sources. H_3^+ will be observed in a great many more

objects with higher spectral resolution. We may not have to wait many years before H_3^+ is observed in extragalactic objects.

5.2 H_3^+ emission

Observing the infrared spectrum of H_3^+ in emission is an interesting possibility. One remembers the strong and pure H_3^+ emission lines observed in planetary ionospheres.⁷ The strongest H_2 quadrupole emission line $\text{S}_1(1)$ (with a spontaneous emission lifetime of 7×10^6 s⁶⁹) is observed with large signal to noise ratios in planetary nebulae,⁷⁰ extragalactic superluminous objects,⁷¹ and many other objects, even using low resolution spectrometers. In order to evaluate the prospects for detecting H_3^+ emission we make a rough estimate of the ratio of intensities for H_3^+ emission, $I_{\text{H}_3^+}$, and H_2 emission, I_{H_2} :

$$\frac{I_{\text{H}_3^+}}{I_{\text{H}_2}} = \frac{[\text{H}_3^+]}{[\text{H}_2]} \frac{k_{\text{H}_3^+}}{k_{\text{H}_2}} \quad (7)$$

where $k_{\text{H}_3^+}$ and k_{H_2} are rate constants for collisional pumping from $v = 0$ to $v = 1$. We estimate that the abundance of H_3^+ should be roughly $[\text{H}_3^+]/[\text{H}_2] \approx 10^{-8}$, which one would think would make the ratio small. However, we must consider the differences in the vibrational pumping mechanisms. The collisional excitation of H_2 by H_2



is performed by a weak physical interaction, in which the translational energy of H_2 must be converted to vibrational energy (V–T transfer) during the short time of the encounter. Resonant V–V transfer cannot contribute, since the number of H_2^* remains the same in the ‘reaction’ $\text{H}_2^* + \text{H}_2 \rightarrow \text{H}_2 + \text{H}_2^*$.

On the other hand, the excitation of H_3^+ is performed by a strong chemical interaction



where asterisks signify vibrational excitation. In this case, the molecules attract each other by the Langevin force, form an activated complex $(\text{H}_3^+)^*$, and then dissociate into H_3^{+*} and H_2 . This reaction is known to have a Langevin rate from a deuterium experiment⁶⁴ and a recent experiment of spin modification.⁷² The branching ratio of reaction (VI) to form H_3^+ or H_3^{+*} is not known but we assume that it is not much different from 1 : 1. Then using the approximate equality between the Langevin rate and the rate of rotational energy transfer (R–R),⁷³ and the rule of thumb⁷⁴ $k_{\text{V-T}}/k_{\text{R-R}} \approx 10^{-5}$, we obtain $k_{\text{H}_3^+}/k_{\text{H}_2} \approx 10^5$. If we use experimental and theoretical $v' = 1 \rightarrow 0$ de-excitation rates⁷⁵ and the principle of detailed balancing, we find that $k_{\text{H}_3^+}/k_{\text{H}_2} \approx 10^5\text{--}10^6$ for $T = 2000\text{--}1000$ K.

Thus we obtain an estimate of $I_{\text{H}_3^+}/I_{\text{H}_2} \approx 10^{-3}\text{--}10^{-2}$. This is a minimum value and will be larger for a molecular cloud with a density higher than the critical density.⁷⁶ In such a high-density environment, the H_3^+ intensity will be increased due to the faster collisional pumping (as H_3^+ has a spontaneous emission time of only ≈ 10 ms⁷⁷), but the H_2 intensity will be limited by the slower rate of spontaneous emission.

Even if $I_{\text{H}_3^+}/I_{\text{H}_2} \approx 10^{-3}$, the detection of H_3^+ emission is a realistic prospect in view of the extremely high observed signal to noise ratios of H_2 emission ($\gtrsim 1000$ at low resolution).

5.3 H_3^+ as an interstellar agent

Interstellar H_3^+ not only plays the central role of the protonator to initiate a network of chain reactions, but also performs other essential functions of interstellar chemistry. For

example, it will mediate conversion of *ortho*-H₂ to *para*-H₂ through the proton hop reaction



and proton exchange reaction

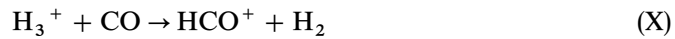


This scrambling of protons will thermalize spin modifications. The actual efficiency of this mechanism should be calculated using the nuclear modification branching ratios theoretically predicted by Quack⁷⁸ and recently experimentally demonstrated.⁷² These processes must be much more efficient than the mechanism proposed earlier⁷⁹



both because of the higher abundance of H_3^+ and the higher rate constant of reactions (VII) and (VIII) than (IX).

Klemperer and Miller⁸⁰ have recently proposed that the strong CO Cameron band emission ($a^3\Pi \rightarrow X^1\Sigma^+$) from 1850–2600 Å observed in the Red Rectangle nebula^{81,82} might be due to a chemical pumping of CO by H_3^+ through the reactions



and



where the asterisk signifies CO in the $a^3\Pi$ excited state. In diffuse clouds where $[e^-] \gg [CO]$, the second reaction is much faster than the first and the rate for CO* excitation is $k_{CO}[H_3^+][CO] \approx 10^{-26} \text{ cm}^{-3} \text{ s}^{-1}$ (here again we neglect the branching ratio between CO and CO*). Glinski *et al.*⁸¹ proposes the direct electron pumping



to be the main mechanism where e^{-*} signifies electrons at high energy $\approx 8\text{--}12 \text{ eV}$. The rate of this process is $k[CO][e^{-*}]$ where the rate constant of excitation k is $\approx 10^{-8} \text{ cm}^3 \text{ s}^{-1}$. Thus the relative efficiency of the H_3^+ pumping of Klemperer and Miller and the electron pumping of Glinski *et al.* depends on the relative magnitudes of $[H_3^+]$ and $10[e^{-*}]$. It is quite probable that H_3^+ is the agent for the emission, especially for the rotationally cold emission core.

We have profited from discussions with W. Klemperer and K. Takayanagi. B.J.M. is supported by the Fannie and John Hertz Foundation. The University of Chicago portion of this work has been supported by NSF grant PHYS-9722691 and NASA grant NAG5-4070.

References

- 1 J. J. Thompson, *Philos. Mag.*, 1911, **21**, 225.
- 2 A. J. Dempster, *Philos. Mag.*, 1916, **31**, 438.
- 3 T. R. Hogness and E. G. Lunn, *Phys. Rev.*, 1925, **26**, 44.
- 4 H. D. Smyth, *Rev. Mod. Phys.*, 1931, **3**, 347.
- 5 H. Eyring, J. O. Hirschfelder and H. S. Taylor, *J. Chem. Phys.*, 1936, **4**, 479.
- 6 J. O. Hirschfelder, *J. Chem. Phys.*, 1938, **6**, 795.
- 7 T. Oka, in *Molecular Ions: Spectroscopy, Structure and Chemistry*, ed. T. A. Miller and V. E. Bondybey, North Holland, New York, 1983, p. 73.
- 8 D. W. Martin, E. W. McDaniel and M. L. Meeks, *Astrophys. J.*, 1961, **134**, 1012.
- 9 T. P. Stecher and D. A. Williams, *Astrophys. Lett.*, 1970, **7**, 59.
- 10 P. M. Solomon and M. W. Werner, *Astrophys. J.*, 1971, **165**, 41.

- 11 T. de Jong, *Astron. Astrophys.*, 1972, **20**, 263. We assume that his Case (A) is closer to reality than Case (B).
- 12 A. E. Glassgold and W. D. Langer, *Astrophys. J.*, 1973, **179**, L147.
- 13 W. D. Watson, *Astrophys. J.*, 1973, **182**, L73.
- 14 W. D. Watson, *Astrophys. J.*, 1973, **183**, L17.
- 15 E. Herbst and W. Klemperer, *Astrophys. J.*, 1973, **185**, 505.
- 16 D. M. Rank, C. H. Townes and W. J. Welch, *Science*, 1971, **174**, 1083.
- 17 D. Buhl and L. E. Snyder, *Nature (London)*, 1970, **228**, 267.
- 18 W. Klemperer, *Nature (London)*, 1970, **227**, 1230.
- 19 T. de Jong, A. Dalgarno and W. Boland, *Astron. Astrophys.*, 1980, **91**, 68.
- 20 E. F. van Dishoeck and J. H. Black, *Astrophys. J. Suppl.*, 1986, **62**, 109.
- 21 H.-H. Lee, R. P. A. Bettens and E. Herbst, *Astron. Astrophys. Suppl.*, 1996, **119**, 111.
- 22 G. Herzberg, *Trans. R. Soc. Can.*, 1967, **V**, 3.
- 23 E. E. Salpeter and R. C. Malone, *Astrophys. J.*, 1971, **167**, 27.
- 24 J. M. MacLeod, L. H. Doherty and L. A. Higgs, *Astron. Astrophys.*, 1975, **42**, 195.
- 25 T. Oka, personal communication.
- 26 A. Dalgarno, E. Herbst, S. Novick and W. Klemperer, *Astrophys. J.*, 1973, **183**, L131.
- 27 W. D. Watson, *Rev. Mod. Phys.*, 1976, **48**, 513.
- 28 T. G. Phillips, G. A. Blake, J. Keene, R. C. Woods and E. Churchwell, *Astrophys. J.*, 1985, **294**, L45.
- 29 E. F. van Dishoeck, T. G. Phillips, J. Keene and G. A. Blake, *Astron. Astrophys.*, 1992, **261**, L13.
- 30 R. T. Boreiko and A. L. Betz, *Astrophys. J.*, 1993, **405**, L39.
- 31 J. K. G. Watson, *J. Mol. Spectrosc.*, 1971, **40**, 536.
- 32 F.-S. Pan and T. Oka, *Astrophys. J.*, 1986, **305**, 518.
- 33 B. T. Draine and D. T. Woods, *Astrophys. J.*, 1990, **363**, 464.
- 34 T. Oka, *Phys. Rev. Lett.*, 1980, **45**, 531.
- 35 T. Oka, *Philos. Trans. R. Soc. London, A*, 1981, **303**, 543.
- 36 T. R. Geballe and T. Oka, *Astrophys. J.*, 1989, **342**, 855.
- 37 P. G. Burton, E. von Nagy-Felsobuki and G. Doherty, *Chem. Phys. Lett.*, 1984, **104**, 323.
- 38 J. H. Black, E. F. van Dishoeck, S. P. Willner and R. C. Woods, *Astrophys. J.*, 1990, **358**, 459.
- 39 J. Tennyson, S. Miller and H. Schild, *J. Chem. Soc., Faraday Trans.*, 1993, **89**, 2155.
- 40 J. P. Maillard, *Spectrochim. Acta, Part A*, 1995, **51**, 1105.
- 41 See for review, T. Oka, *Rev. Mod. Phys.*, 1992, **64**, 1141.
- 42 J. H. Lacy, R. Knacke, T. R. Geballe and A. T. Tokunaga, *Astrophys. J.*, 1994, **428**, L69.
- 43 T. Oka and M.-F. Jagod, *J. Chem. Soc., Faraday Trans.*, 1993, **89**, 2147.
- 44 W. Ketterle, M.-P. Messmer and H. Walther, *Europhys. Lett.*, 1989, **8**, 333.
- 45 J. K. G. Watson, S. C. Foster, A. R. W. McKellar, P. Bernath, T. Amano, F.-S. Pan, M. W. Crofton, A. J. Altman and T. Oka, *Can. J. Phys.*, 1984, **62**, 1875.
- 46 R. Genzel, in *The Galactic Interstellar Medium*, ed. D. Pfenninger and P. Bartholdi, Springer-Verlag, Berlin, 1992, p. 275.
- 47 L. J. Allamandola, in *Galactic and Extragalactic Infrared Spectroscopy*, ed. M. F. Kessler and J. P. Phillips, Reidel, Dordrecht, 1984, p. 5.
- 48 J.-P. Maillard, P. Drossart, J. K. G. Watson, S. J. Kim and J. Caldwell, *Astrophys. J.*, 1990, **363**, L37.
- 49 P. A. M. Dirac, *Proc. R. Soc. London, A*, 1926, **112**, 661.
- 50 For a pedagogical explanation of the relation between the Pauli principle and relativity, see S. Tomonaga, *The Story of Spin*, Univ Chicago Press, Chicago, IL, 1998.
- 51 T. R. Geballe and T. Oka, *Nature (London)*, 1996, **384**, 334.
- 52 S. Lepp, A. Dalgarno and A. Sternberg, *Astrophys. J.*, 1987, **321**, 383.
- 53 T. R. Geballe, F. Baas, J. M. Greenberg and W. Schutte, *Astron. Astrophys.*, 1985, **146**, L6.
- 54 W. A. Schutte, P. A. Gerakines, T. R. Geballe, E. F. van Dishoeck and J. M. Greenberg, *Astron. Astrophys.*, 1996, **309**, 633.
- 55 G. F. Mitchell, J.-P. Maillard, M. Allen, R. Beer and K. Belcourt, *Astrophys. J.*, 1990, **363**, 554.
- 56 B. J. McCall, T. R. Geballe, K. H. Hinkle and T. Oka, manuscript in preparation.
- 57 A. D. McFadzean, D. C. B. Whittet, A. J. Longmore, M. F. Bode and A. J. Adamson, *Mon. Not. R. Astron. Soc.*, 1989, **241**, 873.
- 58 T. R. Geballe, B. J. McCall, K. H. Hinkle and T. Oka, manuscript in preparation.
- 59 W. W. Morgan, H. L. Johnson and N. G. Roman, *Publ. Astron. Soc. Pac.*, 1954, **66**, 85.
- 60 D. C. B. Whittet, A. C. A. Boogert, P. A. Gerakines, W. Schutte, A. G. G. M. Tielens, Th. de Graauw, T. Prusti, E. F. van Dishoeck, P. R. Wesselius and C. M. Wright, *Astrophys. J.*, 1997, **490**, 729.
- 61 B. J. McCall, T. R. Geballe, K. H. Hinkle and T. Oka, *Science*, 1998, **279**, 1910.
- 62 J. H. Black, in *IAU Symp. 120 Astrochemistry*, ed. M. S. Vardya and S. P. Tarafdar, Dordrecht, Reidel, 1987, p. 217.
- 63 T. Amano, *Astrophys. J.*, 1988, **329**, L121.
- 64 V. G. Anicich and W. T. Huntress, Jr., *Astrophys. J. Suppl.*, 1986, **62**, 553.
- 65 J. C. Maxwell, *Philos. Trans. R. Soc.*, 1879, **170**, 231.

- 66 M. P. Langevin, *Ann. Chim. Phys.*, 1905, **5**, 245.
- 67 G. Sundström, J. R. Mowat, H. Danared, S. Datz, L. Broström, A. Filevich, A. Källberg, S. Mannervik, K. G. Rensfelt, P. Sigraý, M. af Ugglas and M. Larsson, *Science*, 1994, **263**, 785.
- 68 E. F. van Dishoeck, in *IAU Symp. 120, Astrochemistry*, ed. M. S. Vardya and S. P. Trafdar, Dordrecht, Reidel, 1986, p. 51.
- 69 J. H. Black and A. Dalgarno, *Astrophys. J.*, 1976, **203**, 132.
- 70 See for example, H. A. Thronson, Jr., *Astrophys. J.*, 1981, **248**, 984.
- 71 See for example, T. R. Geballe, *Can. J. Phys.*, 1994, **72**, 782.
- 72 D. Uy, M. Cordonnier and T. Oka, *Phys. Rev. Lett.*, 1997, **78**, 3844.
- 73 T. Oka, *Adv. Atom. Mol. Phys.*, 1973, **9**, 127.
- 74 W. H. Flygare, *Acc. Chem. Res.*, 1968, **1**, 121.
- 75 M. Cacciatore, M. Capitelli and G. D. Billing, *Chem. Phys. Lett.*, 1989, **157**, 305.
- 76 J. M. Shull and D. J. Hollenbach, *Astrophys. J.*, 1978, **220**, 525.
- 77 G. D. Carney and R. N. Porter, *J. Chem. Phys.*, 1976, **65**, 3547.
- 78 M. Quack, *Mol. Phys.*, 1977, **34**, 477.
- 79 A. Dalgarno, J. H. Black and J. C. Weisheit, *Astrophys. Lett.*, 1973, **14**, 77.
- 80 W. Klemperer and A. Miller, personal communication.
- 81 R. J. Glinski, J. A. Nuth, M. D. Reese and M. L. Sitko, *Astrophys. J.*, 1996, **467**, L109.
- 82 R. J. Glinski, J. T. Lauroesch, M. D. Reese and M. L. Sitko, *Astrophys. J.*, 1997, **490**, 826.

Paper 8/00655E; Received 23rd January, 1998